We are IntechOpen,
the world's leading publisher of Open Access books
Built by scientists, for scientists

6,900
Open access books available

185,000
International authors and editors

200M
Downloads

154
Countries delivered to

Our authors are among the

TOP 1%
most cited scientists

12.2%
Contributors from top 500 universities

CLARIVATE ANALYTICS
BOOK CITATION INDEX
INDEXED

WEB OF SCIENCE™

Selection of our books indexed in the Book Citation Index
in Web of Science™ Core Collection (BKCI)

Interested in publishing with us?
Contact book.department@intechopen.com

Image-Based High-Content Screening in Drug Discovery

Marjo Götte and Daniela Gabriel
Novartis Institutes for BioMedical Research, Basle,
Switzerland

1. Introduction

Immunofluorescence microscopy is a powerful tool for the detection of multiple changes in single cells at sub-cellular level. During the last 10-15 years, confocal and wide-field microscopy have evolved from tedious small scale experiments to medium- or even high-throughput technologies, under the name of high-content screening (HCS). Sample preparation and image acquisition have been automated and several software applications are available for image analysis to obtain quantitative information from the cells. In academia HCS is mainly used in siRNA and cDNA screens to identify genes and proteins involved in specific pathways and processes (Blackmore et al., 2010; Neumann et al., 2010; Pelkmans et al., 2005 as examples). siRNA screens are performed also in pharmaceutical companies for target identification. In addition, in pharmaceutical industry HCS has been adopted as an enabling technology for compound profiling, compound development, secondary screening and even full-deck primary screening (Guzi et al., 2011; Ibig-Rehm et al., 2011; Li et al., 2003; Nadanaciva et al., 2011; Simonen & Gabriel, 2008). The field is still rapidly evolving and new automated cell imagers are coming to the market as well as novel software for image analysis. HCS provides vast amounts of data from each sample and even from each individual cell. During the last years various programs to analyze this data in a multiparametric way have been developed (Gorenstein et al., 2010; Kümmel et al., 2011, Neumann et al., 2010).

Below, the benefits of HCS technology for primary hit finding and secondary screening experiments are discussed. In addition, the technical requirements for high- and medium throughput, the challenges in plate preparation and imaging, image and data analysis and data management are outlined. Examples are provided how to use HCS in primary hit finding campaigns, as well as its use in sophisticated lower-throughput assays using primary cells to generate added value.

2. What are the benefits of high-content screening

Biochemical screens for drug candidates utilize purified proteins in very reductionist assays with the benefit that the compounds can act directly on the target. However, some proteins may not be purified being in their native conformation, sometimes only the catalytic domain of the protein is used in the assay due to problems of producing the full-length protein, and

the substrates are often artificial. When a protein functions in a multiprotein complex it might be difficult or impossible to produce all the subunits and to assemble them in an active complex. Sometimes all the components contributing to a cellular reaction are not even known. Typically biochemical screens are performed to identify inhibitors of kinases, proteases, enzymes and protein-protein interactions.

In cellular assays exploiting genetically non-manipulated cells all the components needed for a reaction are usually present, properly assembled and in physiologically correct stoichiometric relations. However, in cellular screens marker or reporter constructs are often used in cells over-expressing the target. In reporter gene assays (RGAs) the readout is usually indirect and can be far downstream of the actual target. Often reporter genes are not in their natural environment in the genome, and they may contain incomplete regulatory regions. Therefore, RGAs are prone to pick up unspecific compounds. Other cellular screening formats for G protein-coupled receptors (GPCRs) like Ca^{2+} flux assays, homogeneous ELISA assays, bioluminescence resonance energy transfer (BRET) and the numerous luminescence-based assays for cell viability and toxicity are robust, easy and fast to perform. Nevertheless, they provide information about a single parameter only, whereas sub-cellular imaging is able to deliver more content. Multiple parameters like cytoplasm shape, size, area, as well as information about nuclear intensity, size, and shape in addition to the target-specific fluorescence readouts can deliver various insights of the compound's mode of action and unspecific effects early on.

In addition to increased content, another benefit of HCS is to enable screening with assays that were earlier impossible in high throughput, such as trafficking of proteins within cells or morphological changes. Sophisticated image analysis in HCS provides more information from the hits than the traditional screens, cytotoxicity being only one additional feature obtained in HCS assays. HCS enables screening for pathways and phenomena without having a specific target in mind, thereby allowing identification of novel targets. Typical examples of phenotypic screens are stimulation of neurite outgrowth, neuronal survival, autophagy or muscle growth. As in standard cellular screens, also in HCS often genetically manipulated cells are used, but HCS assays can be performed with non-manipulated or primary cells by analyzing changes in endogenously expressed cellular components, which makes the assays physiologically more relevant. Compared to traditional biochemical and cellular screening assays HCS is still slower and usually non-homogeneous. Washing steps are generally required in the staining process and image acquisition takes longer than reading fluorescence or luminescence with plate readers, making HCS more time-consuming and expensive.

We have compared variability and sensitivity of HCS and RGA for the screening of inhibitors for PI3K – Akt – Foxo3A pathway. Both assays were equally reproducible, but the HCS assay had a better statistical quality. The HCS assay was more sensitive than the RGA although it was not able to identify additional chemical scaffolds as hits (Unterreiner et al., 2009). However, this study represents only one HCS assay and one RGA, and the picture might change when comparing more assays.

Since 2005 we have used HCS in primary and secondary screening in numerous projects with varying biology and assay set up. Being convinced about the power of HCS we have recently started to perform also full-deck (>1 million compounds) primary screening with the HCS technology.

3. Technical aspects of HCS

3.1 Cells

Not all cells are equally suited for HCS due to the requirements of microscopic images and image analysis. Large cells, not clumping or growing on top of each other are best suited for automated image analysis. The U-2 OS osteosarcoma cells are an example of a cell line well suited for automated image analysis: The nuclei are well separated from each other allowing determination of the accurate cell number, and the cytoplasm of U-2 OS cells is large enabling sub-cellular image analysis (Fig. 1). HEK293 cells, derived from human embryonic kidney cells, are commonly used in cell biology and in cellular screening, but due to their small size they are less suited for sub-cellular analysis. In small-scale experiments high-resolution objectives might be used, therefore the size of the cells does not limit the experiments as much as in higher throughput assays.
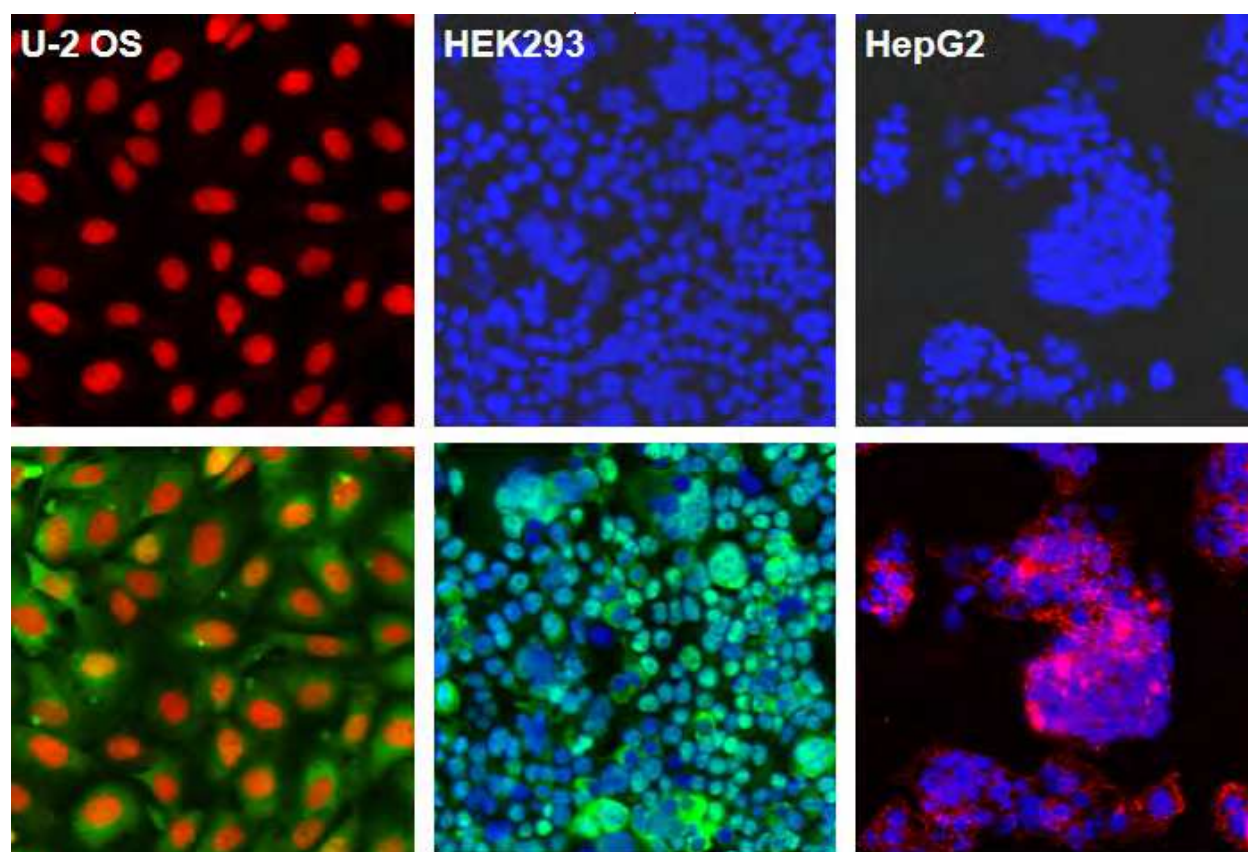

Fig. 1. Examples of some commonly used cell lines with different suitability for HCS. All images are in the same scale and were acquired with IN Cell Analyzer 3000 using the 40x objective. The upper panel images show nuclei stained with different dyes: U-2 OS, red: DRAQ5; HEK293 and HepG2, blue: Hoechst 33342. In the lower panel overlay images are shown using the respective nuclear stain and U-2 OS, green: GFP fusion to a cytoplasmic protein; HEK293, green: cytoplasmic/nuclear protein stained with an antibody; and HepG2, pink: surface receptor stained with an antibody.

For automated image analysis, the cells need to be well separated in order to normalize the signal to cell number to account for changes in cell density by batch to batch variation. Some cells, such as the commonly used hepatocellular carcinoma HepG2 cells, are clumping and it

is difficult to determine the cell number based on the nuclear stain. In addition, the HepG2 cells are small in size (Fig. 1). Suspension cells are also not well suited for HCS due to the potential loss of cells by the washing steps of staining processes. In addition, suspension cells are small allowing measurement of changes in fluorescence intensity but analysis of any sub-cellular compartment is hardly feasible. However, depending on the biology, we have used sometimes also small, clumping and even suspension cells in HCS. In these cases the available readouts in image analysis were limited, but by evaluating different methods to stain the cells and to analyze the images acceptable and satisfactory results could be achieved.

Not only established or recombinant cell lines, but also primary cells, as well as embryonic and induced pluripotent stem cells can be used in HCS assays. The benefit of using genetically non-manipulated cells is that the relevant components of the pathway studied are expressed endogenously at proper expression levels and regulated in an authentic way. Fusion of the target to a fluorescent protein, however, is very convenient in HCS assays, since antibody staining can be omitted. Very often transiently or stably transfected cells are used, whereby the expression and regulation of the fusion protein is at least partly under the control of non-natural elements. Creating knock-in cells, where the fusion protein or the marker is in the natural position in the genome most closely mirrors the endogenous expression and regulation. Generation of cells with disease-relevant mutations with this technique provides excellent cell models for screening (Nilles & London, 2007). Until now most of the cells generated with this approach are either cancer cell lines or of mouse origin. However, the technology for induced pluripotent cells is advancing rapidly, making differentiated human cells with natural disease-relevant mutations available (Park et al., 2008).

3.1.1 Live cell analysis versus fixed cells

For kinetic studies living cells are obviously needed. Several large time-lapse high-content screens have been performed in academia. Such screens provide an advantage when processes like apoptosis, where the cells are responding non-synchronously, are studied (Antczak et al., 2009). Also mitosis, which is a rare event at any given time in a cell population, benefits from a time-lapse analysis (Neumann et al., 2010; Schmitz et al., 2010). To follow live cells over time, either fluorescent proteins are used as markers or the cells are stained with dyes that are tolerated by the cells. In order to analyze all samples with the same time intervals good logistics in sample preparation and imaging is required. The different steps in the whole screening process (cell culture and plating, transfection or compound addition, cell incubation and image acquisition) need to function seamlessly which results in reduced batch sizes in live cell screens.

Cell fixation after compound or siRNA treatment enables decoupling sample preparation and image acquisition. Thereby these two processes do not need to function synchronously, and the fixed plates can be stored at 4°C relatively long times (3-5 days generally, depending on the assay also >5 days) without loss of fluorescence signal. Using assays with fixed cells allows higher throughput at a defined end point. However, such assays provide information on the effect of the analyzed compounds only at a single time point that needs to be carefully evaluated for the screen. We have chosen to fix the cells in our screening campaigns, since this allows us more flexibility in the use of the imagers and the plate

preparation platforms and an increase of batch size. Also, in case of a technical problems, samples are not lost, and can be imaged after solving the technical issues.

3.2 Sample preparation - automation

HCS assays using fixed cells are non-homogeneous with the need of several washing steps, with the number of washing steps depending on the use of fluorescent fusion proteins or antibody labelling. In our screening unit, the vast majority of projects use antibody staining to visualize the target proteins rather than fluorescent fusion proteins. Therefore, we have built automated platforms for fixation, staining and washing steps required by immunostaining protocols. The first platform (Fig. 2A) serves for compound addition to cell plates followed by an incubation step at 37°C for a defined compound incubation time. Thereafter the cells are fixed by e.g. addition of paraformaldehyde using a dispenser, followed by a washing step with a 1536-well plate washer. On the second platform (Fig. 2B) the plates are further processed by dispense of primary and secondary antibodies, followed by incubation and washing steps. In order to gain flexibility compound addition and fixation steps are decoupled from the antibody staining process on separate platforms.

Fig. 2. Plate preparation platforms for automated HCS assays in 384 and 1536-well formats. A) Platform is used for compound addition, incubation and fixation. B) Platform is equipped with robot, dispensers, washers and incubators for automated antibody staining.

When setting up a 1536-well plate high-content assay with an automated plate preparation platform it is critical to test the accuracy (correctness of the transferred volume) and precision (reproducibility) of the plate washers and dispensers, since they have a very high impact on the quality of the HCS assay. Especially for 1536-well dispensers and washers the maintenance and washing procedures are critical to avoid clogging of the pins. The time

needed for plate preparation of an immunostaining assay is much longer than in homogenous assays and the higher number of steps can introduce more errors. Therefore, due to the increase of protocol complexity unattended runs are more challenging.

3.3 Cell imagers

In brief, cell imagers for high-content screening are automated microscopes with automated image analysis. The first automated cell imager came to the market 1997 (Giuliano et al., 1997). Since then, numerous confocal and wide-field imagers have become commercially available. Many of them are, or can be optionally equipped with environmental control for live-cell assays. The instruments are usually equipped with autofocus and an image analysis software is included in the package.

For small and medium-scale experiments the throughput of the instrument is not as crucial; however, for high-throughput screening the following features are important: a) the imager should accept 1536-well plates, b) the speed of image acquisition should be high (20-90 min per 1536 well plate), and c) the hard disk of the instrument should be able to store terabytes of data, or alternatively setup for automated data transfer to a dedicated server.

Imaging speed can be enhanced by acquiring two or even three images on different channels simultaneously. This is possible by using imagers equipped with several cameras. However, due to overlapping emission spectra it is rarely possible to acquire more than two images simultaneously. To achieve reasonable statistics, a certain amount of cells need to be analyzed per treatment or well. This can be achieved by acquiring several images per well which, however, will prolong the imaging process. An improvement is the use of cameras with large field of view to capture a decent number of cells in each single image.

Depending on the assay and throughput, different imagers are optimal for high-content screening. In our unit we have used four different HCS instruments. We started HCS using IN Cell Analyzer 3000 (GE) which is a high-resolution confocal imager equipped with 3 laser lines, 3 CCD cameras with a large field of view and on-the-fly image analysis (simultaneous with image acquisition). It is a fast instrument with user-friendly image analysis software, although unable to read 1536-well plates. In order to perform full-deck HCS campaigns in 1536-well format we setup the Opera QEHS (PerkinElmer) which is a confocal imager equipped with 4 lasers and 4 CCD cameras allowing on-the-fly image analysis with sub-cellular resolution. Thus, Opera is the imager of choice for higher throughput screening campaigns with the need of high resolution. For HCS with medium throughput we use IN Cell Analyzer 2000 (GE) which is wide-field imager equipped with a large-chip CCD camera. It can handle 96-1536 well plates; however, image analysis needs to be done after image acquisition. For high-throughput screening campaigns requiring for example fluorescence intensity measurements without sub-cellular resolution, we utilize the Acumen® ᵉX3 (TTP LabTech), a plate scanning device equipped with three lasers. Also Acumen allows analysis of the distribution of fluorescence intensity on-the-fly (in parallel to scanning). In chapter 4 we give examples of different screening campaigns and devices chosen for different assays.

3.4 Image analysis

To efficiently use the wealth of information within the acquired images the automated microscopes are delivered with image analysis software. In addition, several commercially and freely available third party software packages are available to analyze microscope

images (Carpenter et al., 2006; Gilbert et al., 2009¸ Rämö et al, 2009; Wang et al., 2010). The image analysis programs vary from simple, easy-to-use ready-made modules to writing the image analysis scripts by the user (Niederlein et al., 2009; Pepperkok et al., 2006¸ Swedlow et al., 2003). The former ones make the start of HCS easier for beginners, but the latter offer more flexibility in terms of excluding unwanted structures or defining specific cellular compartments.

For automated image analysis good quality images are required. By size exclusion, dust or larger particles can be filtered out as well as fluorescent particles by fluorescence intensity filter. Sub-cellular analysis is often shown in literature for a single cell as example. When transferred to all cells from a whole well or even to all wells of a 1536-well plate, the algorithm needs to be stable to account for cell populations where size or orientation of the cells may vary. In addition the analysis scripts need to be robust since the intensity of the staining of the cells can vary from well to well due to pipetting procedures.

From a technical point of view, the simplest solution is to use the image analysis software of the imager since no transfer of the images or image conversion step is required. The fastest solution is to analyze images in parallel with image acquisition (on-the-fly image analysis). On-the-fly analysis offers the additional advantage by monitoring the assay quality in a timely fashion that in case of a decreased assay quality, the screener can interact accordingly. Being able to perform image analysis with a computer cluster instead of individual computer(s) would be of great benefit for high-throughput screens to improve analysis speed. Another way to accelerate image analysis is to use multicore computers that can analyze several wells in parallel. However, not all image analysis software packages support multicore analysis.

Not only the provided software coming with the instrument, but also third party software can be used for image analysis. However, each imager creates usually a specific image format with link to metadata (like objective lens used, pixel resolution etc.) which can complicate the use of third party analysis software. Conversion of the images to another format is often required which slows down the whole screening process and usually increases the space needed for image storage. We routinely use the image analysis software provided with the imager, especially for high-throughput campaigns. In few exceptional cases requiring specific algorithms, a third party software with specific features is used for small or medium scale screens.

3.5 Data analysis

To analyse single readouts from HCS campaigns any high-throughput data analysis tool can be used which is able to display heatmaps for plate pattern analysis and to perform dose response curve fitting. The unique requirement for image-based HTS is the generation of a link to the images to rapidly verify whether a hit is a true active or a false positive (Fig. 3). Preferentially the visualization is established in a software package where treatment or compound information is linked.

HCS is able to provide information-rich data sets containing readouts on multiple cellular parameters. In addition to the fluorescence intensity parameters and number of cells, their morphology and the intracellular distribution of cellular proteins can be analysed quantitatively (Loo et al., 2007; Young et al., 2008). To explore the high content of images through multi-parametric data analysis more sophisticated tools are needed. The combination of several parameters can improve the assay quality, however, the statistical

parameter, Z' value, which is commonly used for single readouts needs to be adapted for the analysis of multiple features (Kümmel et al., 2010).
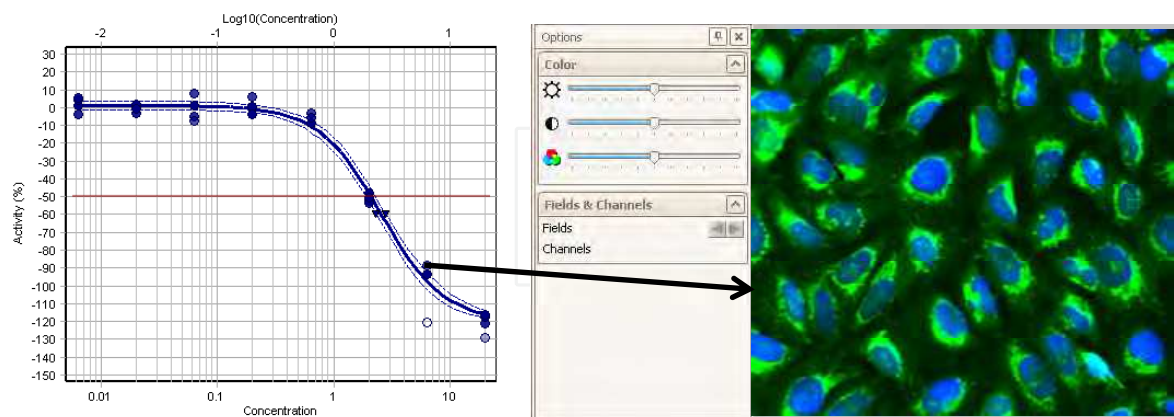

Fig. 3. Example of a concentration response curve fitted in the program to analyze screening data. By clicking an analysis point in a concentration response curve or a well in a heatmap, the respective image is displayed.

In order to enable the analysis of dozens of features in parallel we have generated an in-house software package (Kümmel et al, 2011). Multiple readouts can be either combined to classify samples into hits or inactives or to cluster sample responses into groups similar to control compounds or samples with similar phenotypes (Fig. 4). Such clustering analysis can be used in primary screening for hit identification as well as to cluster hits based on their potency, toxicity or off-target effects.
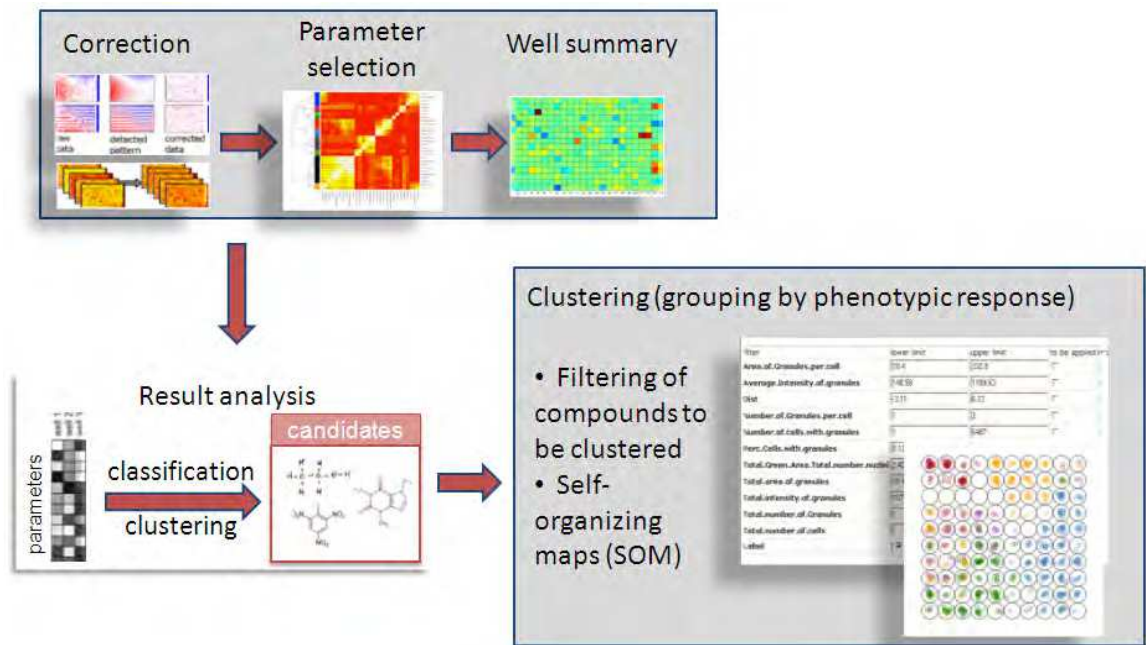
Fig. 4. Analysis of multiparametric HCS data. Data preprocessing consists of correction for plate pattern and plate effects, parameter selection by dimension reduction and well summary. The parameters are being further analyzed by either classification or clustering. Visualization of clustering results in self-organizing maps helps to identify similar phenotypes.

3.6 Data management

Every imager generates its own sometimes proprietary image format, and the format of the data files from each image analysis differs depending on the analysis software used. Therefore, data management and data mining can be problematic when using different imagers or image analysis software packages. With certain image analysis software the data output format might even vary depending on the analysis algorithm applied. To enable the link from image and metadata to the result file can be a challenge due to the variety of formats. In addition, creating software tools enabling the search of plates, compounds, or treatments combined with image and data visualization for comparison of images and data generated by different imagers is still a major challenge.

The high-throughput screening with sub-cellular resolution is focused to specific sites in our company with the consequence of interacting with project teams located in different countries. To allow all team members to view the images irrespective whether they have the specific analysis software or not, we have created a web-based tool to display the images (Fig. 5).
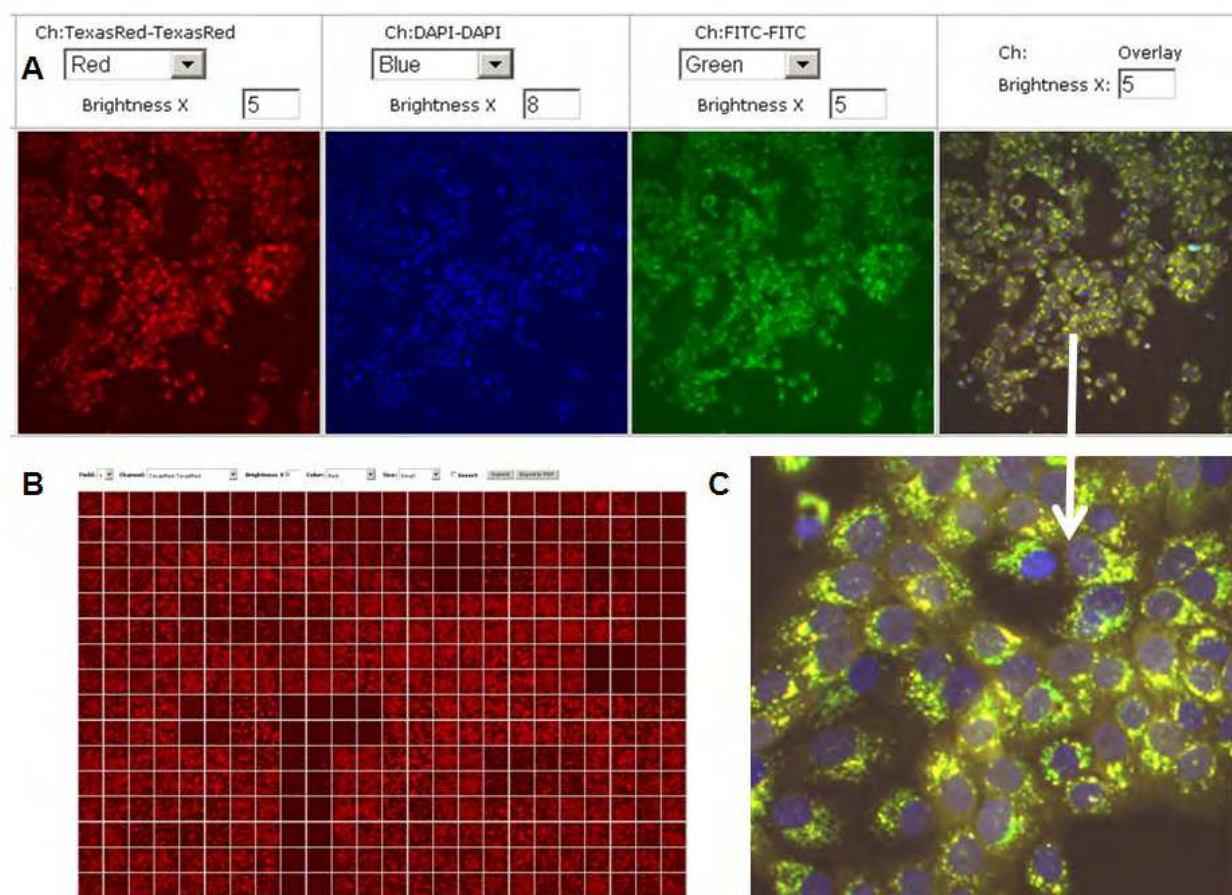

Fig. 5. Visualization of cell images with a web-based tool. Individual wells inspection (A) and whole plate views (B) are possible. In addition images from the respective well or plate view can be explored with higher magnification to visualize details (C).

With this tool individual images as well as an overview of all images on the plate can be visualized, however no analyzed data is being displayed. Currently we are implementing a database where all images and result files are being stored. The visualization in form of

heatmaps will be available for different readouts enabling the comparison of the quality of the respective readouts. A direct link from the heatmap will open the image to check the integrity of the well for a quick verification of the results.
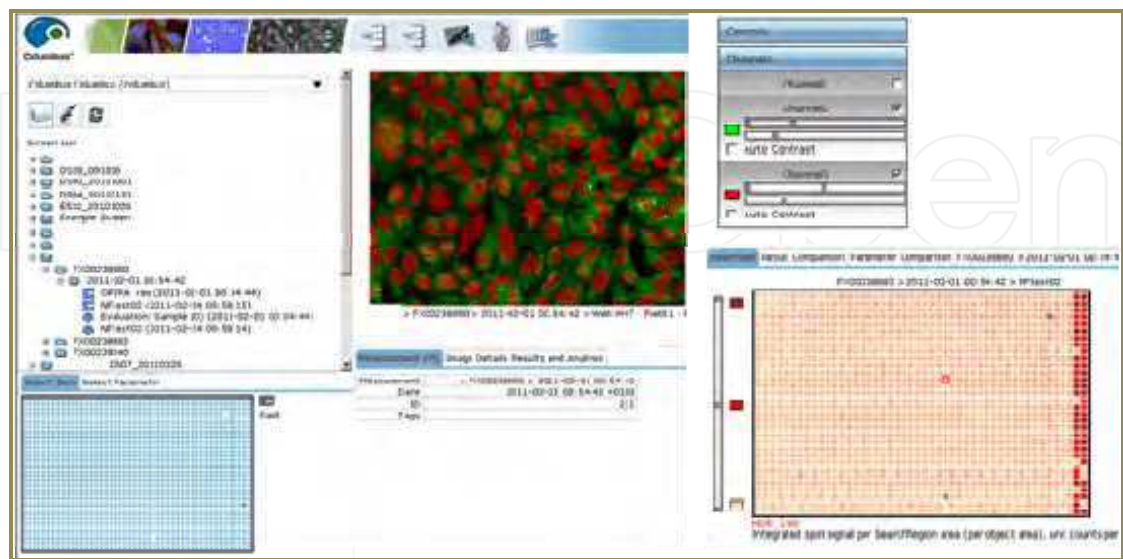

Fig. 6. Visualization of the respective readouts with a link to the images.

4. HCS in primary high-throughput screening

The technologies that have enabled high-content screening in high throughput include plate washers and dispensers for 1536-well plates as well as robot-friendly 1536-well plates suitable for imaging using 10x objectives. Decoupling the plate preparation and imaging processes allows us to exploit all HTS platforms optimally and thereby increase the throughput.

Since we have different instruments in our HCS platform we usually compare image and assay quality and throughput for each project on different readers, and choose the instrument based on the highest quality and throughput. Example projects are described covering high-throughput and medium-throughput campaigns as well as projects with different requirements for resolution.

4.1 HTS for inducers of protein aggregation

As an example, a high-content screening campaign in high throughput to identify compounds inducing protein aggregation within the cytoplasm is described. The sub-cellular analysis of individual cells provided reliable results that could not be reached with any other assay format than high-content imaging. A stable HEK293 cell line was generated overexpressing the protein of interest fused to the HA tag. The detection was based on immunostaining with anti HA antibody followed by a secondary antibody requiring several washing steps. Since HEK293 cells are sensitive to repeated washing steps it was necessary to use poly-D-lysine coated imaging plates which are commercially available.

In this example high-resolution images were needed for the sophisticated image analysis algorithm based on spot detection. Variable spot size with variable intensity was analyzed in the cytoplasmic area which was identified by GFP fluorescence in the cytoplasm. Therefore three colours were imaged with the Opera QEHS, and in order to reach sufficient

quality required for HTS two images were acquired per well using a 20x objective. Imaging and simultaneous image analysis summed up to an imaging time of 90 min per plate. According to the setup of the automated plate preparation system, we were able to process >120 x 1536 well plates per week, however, due to the long imaging time, the throughput was limited to 90 plates per weeks.
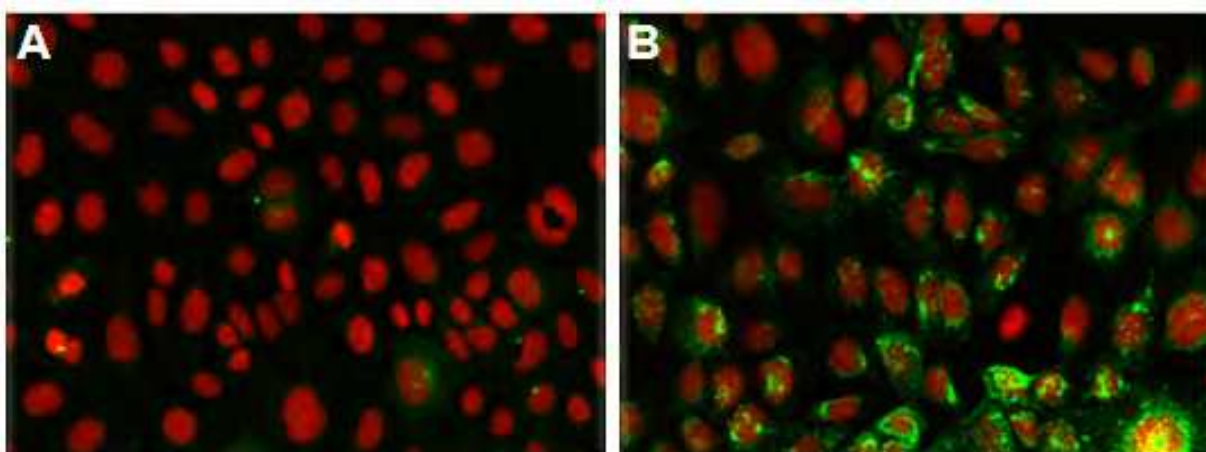

Fig. 7. Protein aggregation in HEK293 cells overexpressing protein of interest tagged with HA-tag (green), nuclear stain Hoechst 33342 (red). A) untreated, B) cells treated with control compound. For better visualization the channel for GFP is not shown and the colours have been changed.

4.2 Medium-throughput screen for granularity

The possibility to quantitatively analyse sub-cellular compartments within the cell is one of the advantages of HCS which makes it for certain projects the unique technique for hit identification. In this example project, the detection of both red and green granules in the cytoplasm of human bladder epithelial cells was aimed for (Fig. 8). For good resolution a 20x objective was required and therefore the use of the laser scanning instrument Acumen was not considered for this project. Long incubation times of the cells made the 1536-well format not suitable and reduced the amount of compounds to be screened to medium throughput.

384-well plates were measured both on the confocal imager Opera QEHS and on the lamp-based imager IN Cell Analyzer 2000 in order to compare image quality and imaging time. Using the 20x objective the image size of Opera images is 430 x 345 µm, whereas the IN Cell Analyzer 2000 has a large field of view camera which results in 760 x 760 µm images. Thus, for imaging the same number of cells two images per well and almost double the imaging time was required with Opera compared to IN Cell Analyzer 2000. Lowering the number of cells imaged had a negative impact on assay quality. Therefore, in this particular assay the imaging time with Opera was 40 min longer per plate already taking into account the ability to acquire images on two channels simultaneously (Table 1).

4.3 Measurement of fluorescence intensity

In most projects high-resolution images are needed for sub-cellular analysis, but in some projects low-resolution images provide adequate results and assay quality. This is especially true for assays where fluorescence intensity is the main readout. In a high-throughput

screening campaign we were looking for compounds inhibiting post-translational modification of a protein localized in the nucleus of a prostate cancer cell line. We monitored two different post-translational modifications simultaneously using antibody staining and measuring the fluorescence intensity in the nuclear region. The images taken with Opera QEHS are shown in Fig. 9. The resolution requirements of fluorescence intensity measurement are in general not very high, therefore imaging with the Acumen was considered for this project.

Opera and Acumen provided qualitatively comparable results in 1536-well format in terms of signal to baseline ratio and Z' values, with the Acumen being much faster with 30 min versus 90 min imaging time with Opera (Table 2). In this specific project the cells needed to be plated at low density, therefore the lower resolution of the Acumen was counterbalanced by the improved statistical quality due to the ability to read the whole well by Acumen (Fig 10).

Primary hit finding was performed using the Acumen whereas the follow-up in concentration-response-curves was done with Opera QEHS to allow the possibility of checking the images for specific compound effects. The reduced imaging time as well as the reduced amount of data storage of the Acumen is an advantage for high-throughput screening in cases where lower resolution is acceptable.
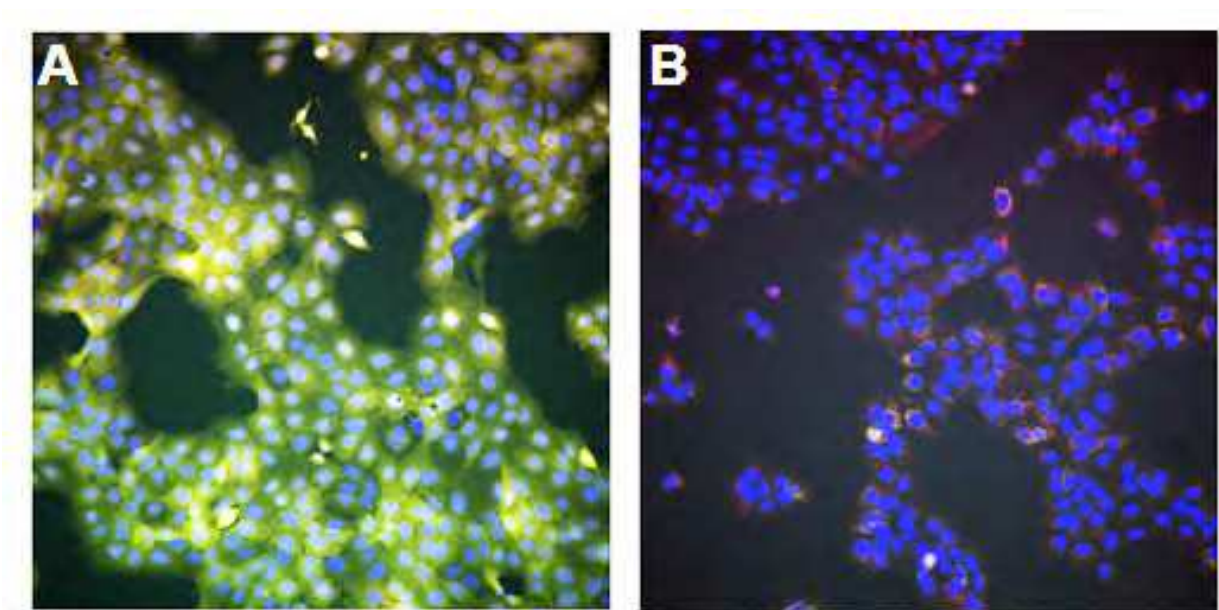

Fig. 8. Granule detection in RT112 cells (human bladder epithelial cells) stably expressing GFP (green) and mCherry fusion proteins (red). Nuclei are stained with Hoechst 33342 (blue). A) untreated, B) cells treated with control compound.

384-well plates, 20x objective, 3 colours	**Opera**	**IN Cell 2000**
	2 images / well	1 image / well
Measurement time / plate	100 min	60 min

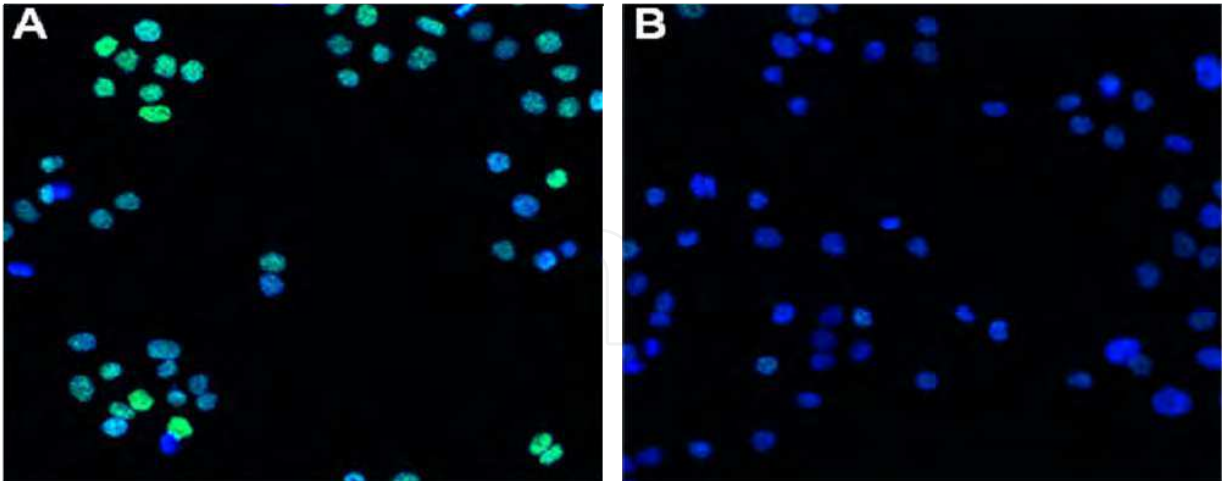Table 1. Overview of imaging time of Opera and IN Cell 2000 for granularity measurement

Fig. 9. Images for fluorescence intensity measurement acquired with Opera. DU145 cells (human prostate cancer cells) stained with Antibody B (green), nuclear stain (blue). For better visualization only two colours are shown in the overlay images. A) untreated, B) cells treated with control compound.
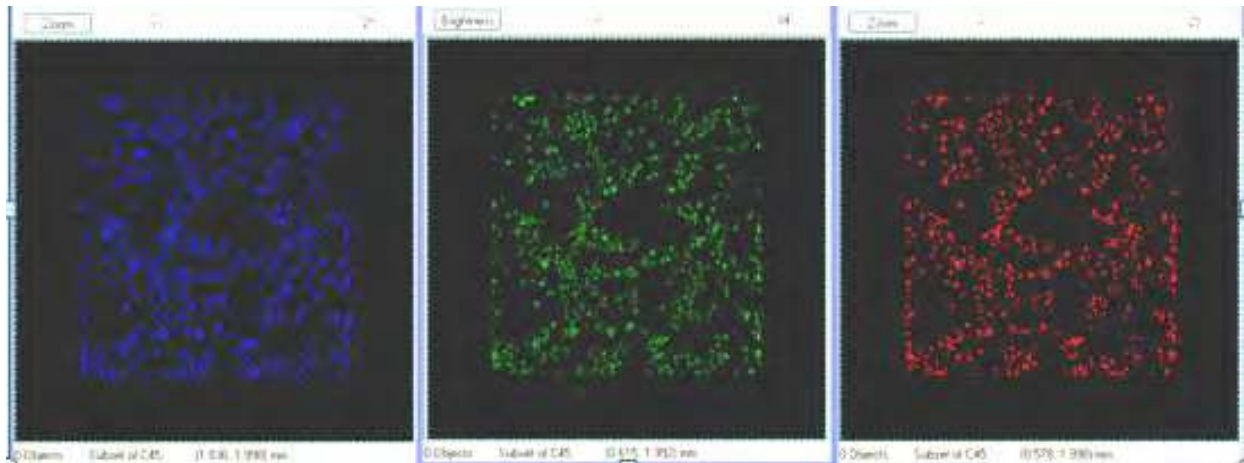

Fig. 10. Fluorescence intensity measurement with Acumen. DU145 cells (human prostate cancer cells) stained with nuclear stain (blue), antibody A (green), antibody B (red).

	Opera	Acumen
1536-well plates, 3 colours	20x objective, 2 images / well	whole well
Measurement time / plate	90 min	30 min

Table 2. Overview of imaging time of Opera and Acumen for fluorescence intensity measurement.

4.4 Analysis of nuclear translocation

Nuclear translocation assays can deliver functional readouts without the side effect of generating many false positives as other conventional assay formats might comprise. Having the advantage of observing the compounds effect on the cells, we decided to screen for small molecules inhibiting the translocation of a protein to the nucleus in U-2 OS cells overexpressing a GFP fusion protein. Since both Opera and Acumen are able to measure nuclear translocation, both were compared for quality and throughput. The assay was quite robust and did not require a very high resolution for the image analysis. Both instruments were able to provide good assay quality in 1536-well format. The plate measurement time was 25 min both with Acumen and with Opera. A 10x objective was used on the Opera and the images were acquired on two channels simultaneously. The applied image analysis on Opera needed longer than the effective imaging time and would have reduced the throughput. However, after streamlining the algorithm, the time of physical imaging and image analysis matched.

Since the confocal images by Opera provide more information on the samples than a plate scanner, the Opera was chosen as the screening instrument for that particular project.
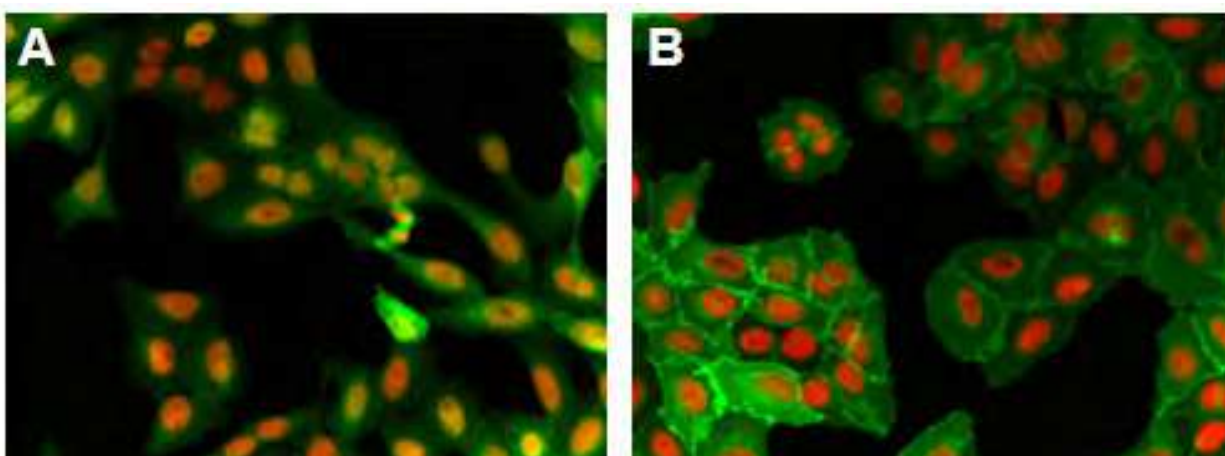

Fig. 11. Translocation of GFP-fusion protein from nuclear region upon small molecule addition. Image analysis is based on the fluorescence intensity in the nuclear area compared to cytoplasm. U-2 OS cells overexpressing GFP fusion protein (green), nuclear stain DRAQ5 (red). A) untreated, B) cells treated with control compound.

4.5 Overview of selected imaging projects

Four different examples are described above with varying requirements for resolution and therefore different choices of imagers for screening. Every assay is optimized for lowest imaging time and highest throughput without loss of quality. Imaging time can vary strongly between 25 to 90 min per 1536 well plate as shown in Table 3.

However, optimizing the imaging time alone is often not sufficient to run a HCS in high throughput; also the immunostaining procedure can be a bottleneck. Antibody staining is much more time consuming than working with GFP fusion proteins since several washing steps are required. To speed up and simplify the staining process the fixative can be added directly to the cell medium, blocking buffer and permeabilization reagent can be combined in one step as well as the nuclear stain added together with the secondary antibody.

Project	Imager	Plate format	Cells	No of compounds screened	Colours	Images/well	Objective	Imaging time/plate (min)
Protein aggregation	Opera	1536	Hek293	>1 mio	3	2	20 x	**100**
Fluorescence intensity	Opera	1536	HEK293	550k	2	2	20 x	**55**
Nuclear translocation	Opera	1536	U-2 OS	>1 mio	2	1	10 x	**25**
Fluorescence intensity	Acumen	1536	DU145	>1 mio	3	whole well	Ca 10x	**30**
Granule detection	IN Cell 2000	384	RT112	20k	3	1	20 x	**60***
Protein aggregation	Opera	384	U-2 OS	25k	2	4	20 x	**30***

Table 3. List of high-throughput assays with different requirements and the effect on the imaging time. * The imaging time needs to be multiplied with 4 in order to compare with imaging of 1536-well plates.

4.6 Technical issues in high-throughput HCS

The time consuming plate preparation process in addition to imaging time (up to several days) can result in delayed quality control measures to detect errors in cell plating or compound distribution. This can be a major issue if undetected failures of batch preparation can only be reported back after a week.

Since the imaging can be of long duration (90 min or more per plate) the 1536-well plates need to be stored in an incubator at 4 °C to prevent evaporation. Nevertheless, before imaging an intermediate step should be calculated to accommodate the plates to room temperature to avoid condensation, therefore we have introduced a 30 min incubation time at room temperature before imaging. Storing fixed and stained plates at 4 °C will allow a later use of the plates for imaging. This decoupled process is beneficial in case of a failure of the plate preparation systems. We observed that although antibacterial agents were added, contaminations can occur with plate storage for longer than two weeks.

Due to small volumes of reagents and the use of common, frequently opened incubators we experienced strong edge effects on 1536-well plates. We were able to compensate that partially with higher volumes of medium or buffer during the incubation steps and using dedicated incubators that are less frequently opened. With a specifically designed 1536-well plate comprising a tightly closing lid (labyrinth lid) evaporation can be mitigated (Pfeifer and Scheel, 2009). In addition, the performance of the plate washers and dispensers needs to be monitored continuously since the washing and dispensing steps are essential for a good performance. The 1536-well dispensing or washing devices have tiny pins which are prone to clogging. Therefore a regular cleaning procedure with detergent, water and ethanol after every use is necessary which leads to a limit in unattended use of the automation systems. Furthermore, working with 1536-well plates often requires shaking to distribute the added reagents evenly. We have added a high-speed shaking step after each reagent addition to our protocol.

5. HCS in small-scale analysis

In contrast to high-throughput assays, where automation-friendly assays and high speed of imaging and image analysis are of utmost importance, in small-scale analysis more complex assay formats are possible. Assay protocols requiring manual or semi-manual steps can be used and precious primary cells, such as neurons, even co-cultures can be used (Anderl et al., 2009). The ability to use primary cells and analyze endogenous proteins can be of great benefit which is enabled by antibody labelling and the sensitivity of confocal imaging. Also several components can be stained in parallel, and to improve the statistical quality of the assay, several images on different channels can be acquired when speed is not the most critical factor. A thorough image and data analysis for also non-expected features can be performed to obtain all possible information from the cells after different treatments.

We have used low and medium-throughput high-content assays to analyze cellular neurotoxicity, neurite outgrowth and neuronal survival. Using primary rat cerebellar granule neurons (CGNs) we developed an imaging assay that has been used in medium throughput to study neurotoxicity (Götte et al., 2010) and neurite outgrowth-promoting activity of low-molecular weight compounds (see below) or proteins (Yan et al,. 2009). The rat cerebellar granule cells can be prepared from a litter of 7-8 pups in 3 h, and the amount of cells obtained allows analysis of 2500 samples in 96-well format and 12.500 samples in 384-well format. The cells can be frozen without loss of viability or ability to grow neurites. Thereby assays with even higher throughput are possible. The intactness of the neuritic network in a high-content assay proved out to be a sensitive measure for cellular neurotoxicity, revealing compound toxicity that was not detected in non-HCS assays or in neuroblastoma cells (Götte et al., 2010). The HCS assay was used to analyze cellular neurotoxicity of compounds whose targets were expressed in the brain.

We have also used the CGNs to study neurite outgrowth in small-scale assays. The neurite outgrowth assay was first developed and validated using the brain-derived neurotrophic factor (BDNF) whose receptor, TrkB, is expressed in the developing CGNs (Segal et al., 1995). Images were acquired with IN Cell Analyzer 3000 and image analysis revealed that BDNF enhanced neurite outgrowth dose-dependently. Additional analysis of the images with a third party software, Neurite Analysis module of HCA-Vision, that is specifically designed to analyze neuronal cultures, revealed that the enhanced neurite outgrowth was rather due to increased branching and increased number of neurites per neuron than increased length of the neurites (Wang et al., 2010). Such detailed information of neuronal morphology can be obtained only from an imaging assay.

We tested the ability of other neurotrophins to promote neurite outgrowth or neuronal survival. Therefore, the CGNs were incubated for 3 days with the neurotrophins, then fixed and stained with the nuclear marker Hoechst 33342 and anti β-tubulin III antibody to specifically label neurons (Lewis and Cowan, 1988). Images were acquired with IN Cell Analyzer 3000 and analyzed with IN Cell 3000 Neurite Outgrowth module for various readouts in respect to neurite area and length (Fig 12). BDNF (10 ng/ml) served as a positive control.

Image analysis revealed that the TrkB ligands, BDNF and NT-4, increased the total number of cells in the culture significantly, suggesting that they have a cell survival-promoting effect (Fig. 12). NT-4 and BDNF enhanced also neurite outgrowth significantly, as seen by the increase of neurite length and neurite area per cell. NT-4 was the most potent neurotrophin enhancing neurite number and branching as analyzed additionally with the HCA-Vision

software. NT-3 enhanced neurite outgrowth modestly and only at high concentrations. The preferred receptor for NT-3 is TrkC which is expressed in the CGNs at a lower level than TrkB (Segal et al., 1995), and accordingly, NT-3 had a slight positive effect on cell survival and neurite outgrowth. NT-3 also enhanced the number of neurites at high concentration (Fig. 12) whereas NGF had no effect on either cell survival or neurite outgrowth. This is in accordance with other published data (Courtney et al., 1997; Nonomura et al., 1996), and our own quantitative RT-PCR results indicating very low expression of the NGF receptor, TrkA in the CGNs (not shown). Thus, the high-content assay was able to reveal expected effects of known neurotrophins validating the assay setup.
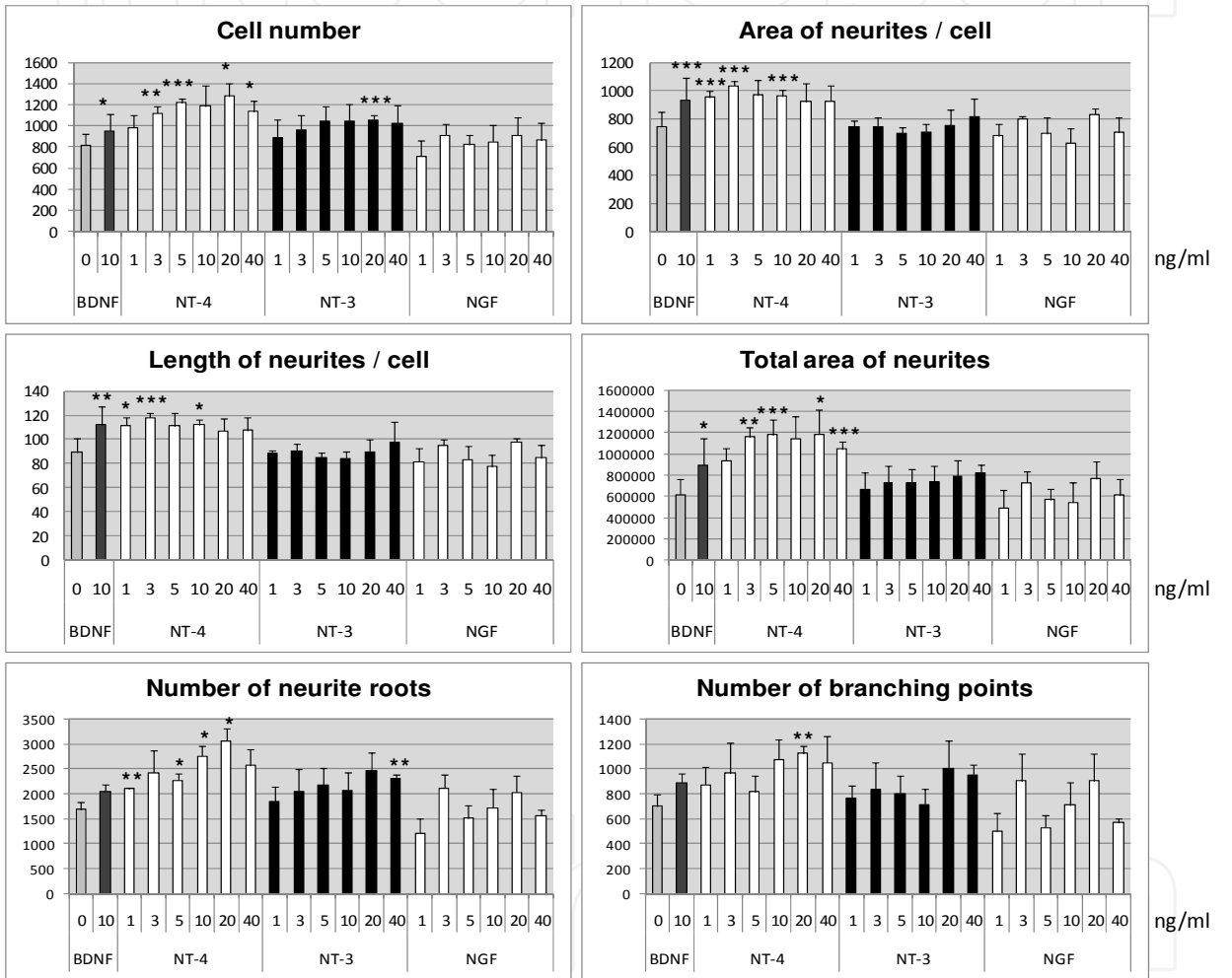
Fig. 12. Effect of neurotrophins NT-4, NT-3 and NGF on cell survival and neurite outgrowth. CGNs from 7 day old rats were incubated with the neurotrophins for 3 days before fixation and staining. Average and standard deviation of triplicate samples are shown. Area and length of neurites are in pixels; pixel size is 0.6 μm. Statistical significance in comparison to DMSO control; ***, p <0.001; ** p<0.01; * p<0.05 in Student' two-tailed paired *t*-test.

The goal was to identify low-molecular weight compounds mimicking the effect of neurotrophins. Several antidepressants have been reported to activate the TrkB pathway *in vivo* (Rantamäki et al., 2007). Therefore, we were interested to test the effect of selected antidepressants on neurite outgrowth of the CGNs expressing TrkB. Three of the nine tested

antidepressants enhanced neuronal survival and/or neurite outgrowth significantly. In addition, image analysis was able to reveal differences in the effects among the three active drugs.

Citalopram induced the most pronounced, concentration-dependent neurite outgrowth by enhancing significantly cell survival and the percentage of neuronal cells in the culture (Fig. 13). Neurite outgrowth and percentage of neurons were increased by imipramine up to 1 μM (Fig. 13.), however, at higher concentration neurite outgrowth was reduced, which could indicate cytotoxicity. Fluoxetine did not enhance cell survival but it enhanced neurite outgrowth at low concentrations. At high concentration (10 μM) fluoxetine was toxic reducing total cell number and percentage of neuronal cells and inhibiting neurite outgrowth almost completely.

The advantage of HCS over assays that analyze total amounts of markers, such as β-tubulin III or neurofilament, is that the effect on cell survival and neurite outgrowth can be distinguished. The enhancing effect of fluoxetine on neurite outgrowth, for example, would probably remain undetected in an assay analyzing merely the total amount of β-tubulin due to the fact that fluoxetine slightly reduced the cell number as compared to the DMSO control.
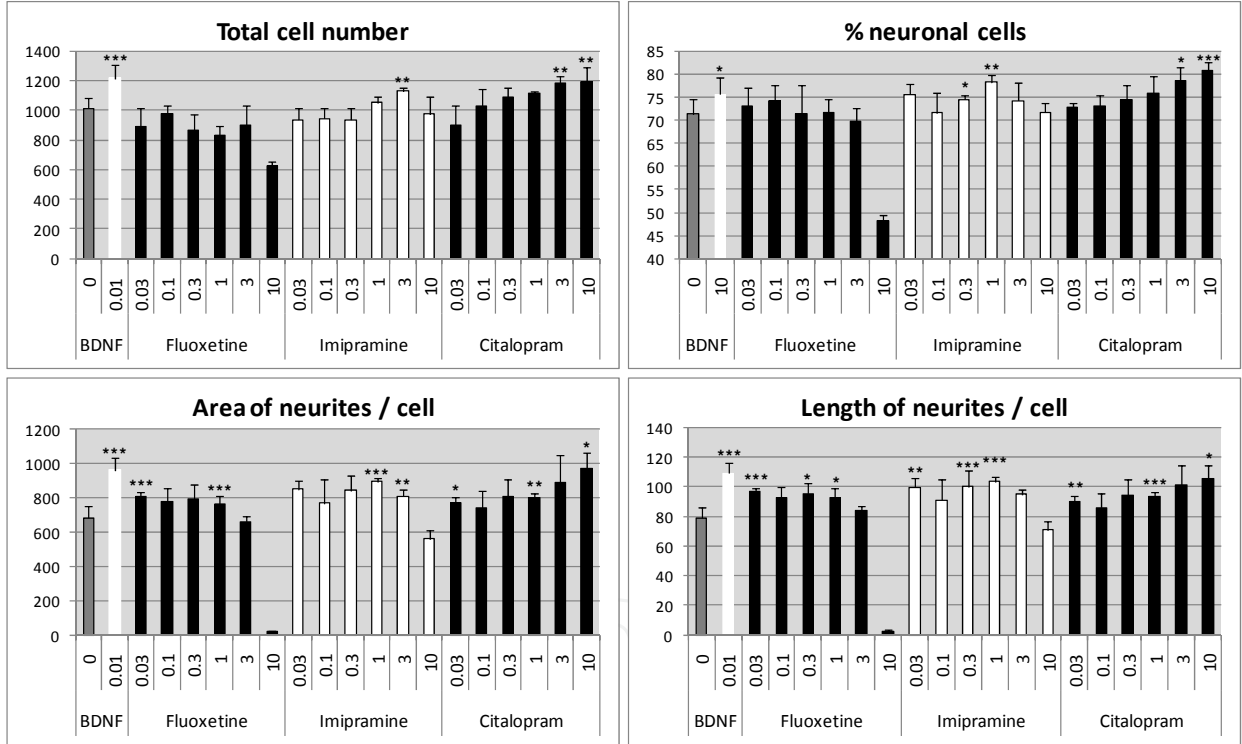
Fig. 13. Effect of fluoxetine, imipramine and citalopram on cell survival and neurite outgrowth. Average and standard deviation of triplicate samples are shown. The concentration of BDNF was 10 ng/ml. The concentrations of the antidepressants are in μM. Area and length of neurites are in pixels; pixel size is 0.6 μm. Statistical significance in comparison to DMSO control; ***, p <0.001; ** p<0.01; * p<0.05 in Student' two-tailed paired t-test.

In small-scale experiments, such as the study of the effect of neurotrophic factors and the antidepressants on neurite outgrowth, an extra colour can be afforded to reveal additional effects of the drugs. In our example, the CGN samples were stained additionally with an

antibody against TrkB which uncovered an interesting, unexpected phenomenon. TrkB was found to localize to the cell bodies and neurites. TrkB was also found in the tips of the growing neurites but only when the cells were cultivated in the absence of a TrkB ligand. The presence of the TrkB ligands BDNF or NT-4, caused disappearance of the TrkB receptor from the tips (Fig. 14).
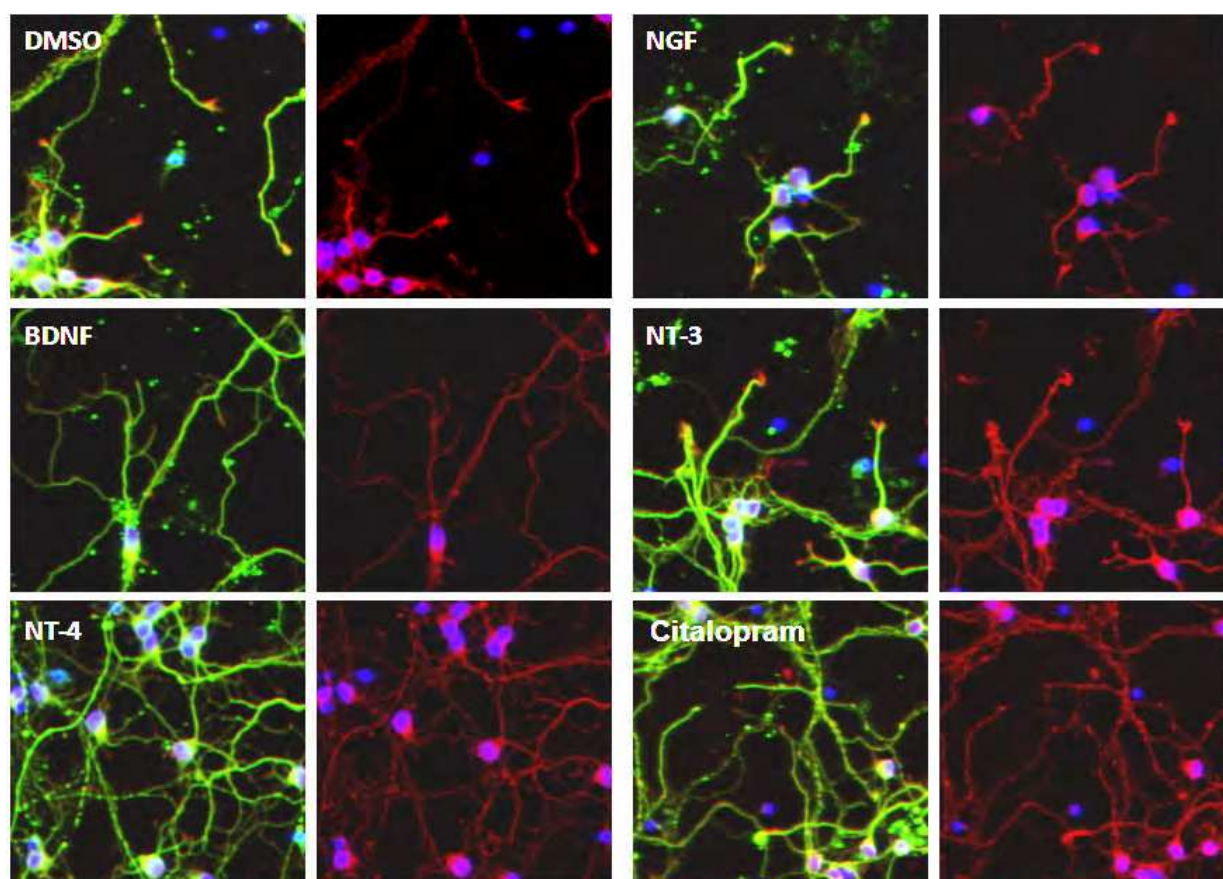

Fig. 14. TrkB ligands and citalopram reduce localization of TrkB to the tips of the neurites. Rat CGNs from 7-8 day old pups were incubated for 3 days with the neurotrophins, DMSO or citalopram, then fixed, stained and images were acquired with IN Cell Analyzer 3000. Red, anti TrkB; green, anti β-tubulin III; blue, nuclei.

In order to quantify TrkB specifically in the tips of the neurites, the neurites were first traced semi-manually with the help of the β-tubulin III staining and using the Imaris® software (Bitplane AG, Zurich, Switzerland). Then the tips were marked as regions of interest (Fig. 15), and the area and intensity of TrkB staining in the marked tips were calculated with a customized MATLAB code. The quantification of TrkB in the tips of the neurites confirmed the visual observation that indeed the TrkB ligands BDNF and NT-4 reduced TrkB in the tips, whereas NGF did not. Surprisingly, also one of the antidepressants, citalopram, caused disappearance of TrkB from tips of the neurites. Whether this is a direct effect of citalopram or whether it stimulates secretion of BDNF which then causes the internalization of TrkB, remains to be studied. Anyhow, this is an example that an additional staining and careful image analysis can reveal unexpected effects of the compounds, and in this special case can help to reveal the mode of action of the active compounds.
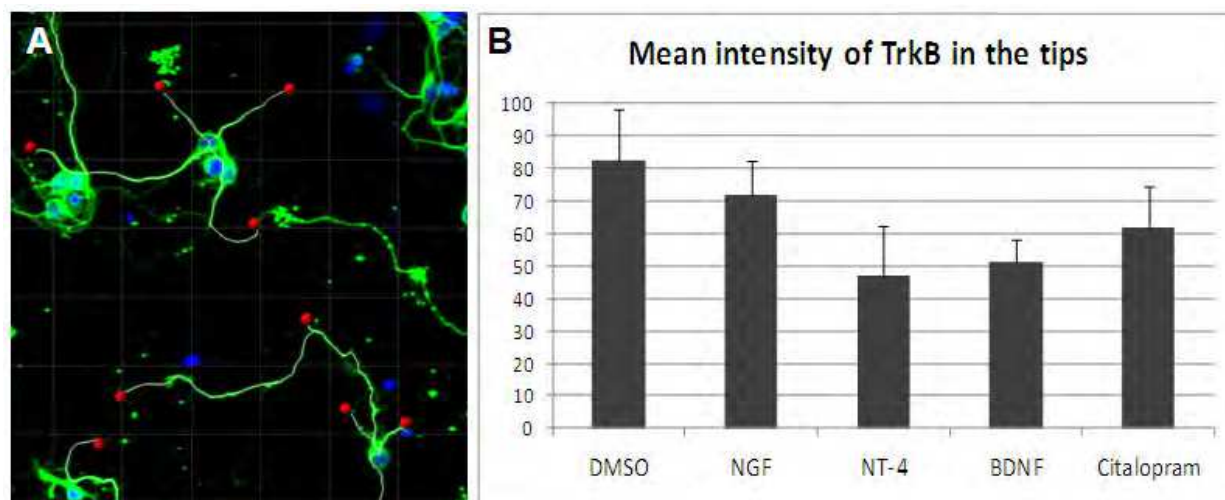
Fig. 15. Quantification of TrkB in the tips of the neurites. A, Image with regions of interest (red) where intensity and area of TrkB staining was measured. Green, β-tubulin staining; blue, nuclei stained with Hoechst 33342. B, intensity of TrkB staining in the tips as analyzed with a MATLAB code. For each condition 29-62 neurites were analyzed.

6. Outlook

The HCS field is developing in two directions. On one hand more sophisticated assays are being developed and more complex biological systems are being exploited, such as stem cells (embryonic, adult, IPS), primary cells, co-cultures, and even tissues and worms like *C. elegans* are quantitatively analyzed. This development is being enabled by improved image analysis software packages for co-cultures or label-free samples.

On the other hand HCS is rendered possible for real high-throughput screening in primary hit finding campaigns through instruments with 1536-well capabilities combining high imaging speed and resolution. Robust assays required for primary hit finding are being developed and sophisticated image analysis packages allow fast, on-the-fly image analysis for real time quality control.

Novel imagers with adjustable confocality and large field of view, which have recently become available, will increase the flexibility and throughput of high-content assays. Hard- and software for sub-cellular imaging are developing for more modular use of the equipment to allow increased diversity of applications, including live-cell imaging with environmental control and even fast kinetics with reagent additions. The analysis of the generated multiparametric data is further emerging and different ways to analyze the vast HCS data are being exploited, with an increasing number of available tools for data visualization.

7. Summary

HCS is an established but still evolving technology in drug discovery. HCS enables in primary screening and compound profiling novel assay formats which were earlier impossible in higher throughput. In addition, sub-cellular imaging is able to deliver more content through multi-parametric data analysis of shape, size, and area in addition to the target-specific fluorescence readouts. There are biological requirements for successful HCS

campaigns including well separated cells as well as dedicated algorithms for the respective image analysis. HCS in high throughput requires automated platforms for sample preparation, high-speed imagers and data analysis software with a dedicated IT infrastructure to manage and mine the wealth of data produced. Primary hit finding can be performed in medium to high throughput with a variety of biological readouts based on sub-cellular imaging, including protein aggregation, granularity detection or translocation events. In lower throughput follow-up assays, sub-cellular imaging can be applied to thoroughly analyze compound effects on primary cells and to reveal additional, unexpected effects. At this point it is too early to evaluate the impact of HCS in novel drugs, whether they are improved in having less undesired side-effects, or developed faster, or whether the attrition rate at late phases would be decreased.

8. Acknowledgement

9. References

Anderl, J.L., Redpath, S. & Ball, A.J. (2009) A neuronal and astrocyte co-culture assay for high content analysis of neurotoxicity. *J. Vis. Exp*. Vol. 5, No. 27, p. 1173.

Antczak, C., Takagi, T., Ramirez, C.N., Radu, C. & Djaballah, H. (2009) Live-cell imaging of caspase activation for high-content screening. *J. Biomol. Screen.*, Vol. 14, No. 8, pp. 956-969.

Blackmore, M.G., Moore, D.L., Smith, R.P., Goldberg, J.L., Bixby, J.L. & Lemmon, V.P. (2010) High content screening of cortical neurons identifies novel regulators of axon growth. *Mol. Cell. Neurosci.*, Vol. 44, No. 1, pp. 43-54.

Carpenter, A.E., Jones, T.R., Lamprecht, M.R., Clarke, C., Kang, I.H., Friman, O., Guertin, D.A., Chang, J.H., Lindquist, R.A., Moffat, J., Golland, P. & Sabatini, D.M. (2006) CellProfiler: image analysis software for identifying and quantifying cell phenotypes. *Genome Biol.*, Vol. 7, No. 10, pp. R100-R100.11.

Courtney, M.J., Åkerman, K.E.O. & Coffey, E.T. (1997) Neurotrophins protect cultured cerebellar granule neurons against the early phase of cell death by a two-component mechanism. *J. Neurosci.*, Vol. 17, No. 11, pp. 4201-4211.

Gilbert, D.F., Meinhof, T., Pepperkok, R., & Runz, H. DetecTiff©: A novel image analysis routine for high-content screening microscopy. (2009) *J. Biomol. Screen.*, Vol. 14, No. 8, pp. 944-955.

Giuliano, K., DeBiasio, R., Dunlay, T., Gough, A., Voloska, J., Zock, J., Pavlakis, G.N. & Taylor, D.L. (1997) High-content screening: a new approach to easing key bottlenecks in the drug discovery process. *J. Biomol. Screen*. Vol. 2, No. 4, pp. 249-259.

Gorenstein, J., Zack, B., Marszalek, J.R., Bagchi, A., Subramaniam, S., Carroll, P. & Elbi, C. (2010) Reducing the multidimensionality of high-content screening into versatile powerful descriptors. *Biotechniques*, Vol. 49, No. 3, pp. 663-665.

Götte, M., Hofmann, G., Michou-Gallani, A-I., Glickman, J.F., Wishart, W. & Gabriel, D. (2010) An imaging assay to analyze primary neurons for cellular neurotoxicity. *J. Neurosci. Methods*, Vol. 192, No. 1, pp. 7-16.

Guzi, T.J., Paruch, K., Dwyer, M.P., Labroli, M., Shanahan, F., Davis, N., Taricani, L., Wiswell, D., Seghezzi, W., Penaflor, E., Bhagwat, B., Wang, W., Gu, D., Hsieh, Y., Lee, S., Liu, M. & Parry, D. (2011) Targeting the Replication Checkpoint Using SCH 900776, a Potent and Functionally Selective CHK1 Inhibitor Identified via High Content Screening. *Mol. Cancer Ther.*, Vol. 10, No. 4, pp. 591-602.

Ibig-Rehm, Y., Götte, M., Gabriel, D., Woodhall, D., Shea, A., Brown, N.E., Compton, T. & Feire, A.L. (2011) High-content screening to distinguish between attachment and post-attachment steps of human cytomegalovirus entry into fibroblasts and epithelial cells. *Antiviral Res.*, Vol. 89, No. 3, pp.246-256.

Kümmel, A., Gubler, H., Gehin, P., Beibel, M., Gabriel, D. & Parker, C.N. (2010) Integration of Multiple Readouts

into the Z' Factor for Assay Quality Assessment. *J. Biomol. Screen.*, Vol. 15, No. 1, pp. 95-101.

Kümmel, A., Selzer, P., Beibel, M., Gubler, H., Parker, C.N. & Gabriel, D. (2011) Comparison of multivariate data analysis strategies for high-content screening. *J. Biomol. Screen.*, Vol. 16, No. 3, pp. 338-347.

Lewis, S.A., Cowan, N.J. (1988) Complex regulation and functional versatility of mammalian alpha- and beta-tubulin isotypes during differentiation of testis and muscle cells. *J. Cell. Biol.*, Vol. 106, No. 6, pp. 2023-2033.

Li, Z., Yan, Y., Powers, E.A., Ying, X., Janjua, K., Garyantes, T. & Baron, B. (2003) Identification of gap junction blockers using automated fluorescence microscopy imaging. *J. Biomol. Screen.*, Vol. 8, No. 5, pp. 489-499.

Loo, L. H., Wu, L. F. & Altschuler, S. J. (2007) Image-based multivariate profiling of drug responses from single cells. *Nat. Methods.*, Vol. 4, No. 5, pp. 445–453.

Nadanaciva, S., Lu, S., Gebhard, D.F., Jessen, B.A., Pennie, W.D. & Will, Y. (2011) A high content screening assay for identifying lysosomotropic compounds. *Toxicol. In Vitro*, Vol. 25, No. 3, pp. 715-723.

Neumann, B., Walter, T., Hériché, J.K., Bulkescher, J., Erfle, H., Conrad, C., Rogers, P., Poser, I., Held, M., Liebel, U., Cetin, C., Sieckmann, F., Pau, G., Kabbe, R., Wünsche, A., Satagopam, V., Schmitz, M.H., Chapuis, C., Gerlich, D.W., Schneider, R., Eils, R., Huber, W., Peters, J.M., Hyman, A.A., Durbin, R., Pepperkok, R. & Ellenberg, J. (2010) Phenotypic profiling of the human genome by time-lapse microscopy reveals cell division genes. *Nature*, Vol. 464, No. 7289, pp. 721-727.

Niederlein, A., Meyenhofer, F., White, D. & Bickle, M. (2009) Image analysis in high-content screening. *Comb. Chem. High Throughput Screen.* Vol. 12, No. 9, pp. 899-907.

Nilles, K.M. & London, B. (2007) Knockin animal models of inherited arrythmogenic diseases: what have we learned from them ? *J. Cardiovasc. Electrophysiol.*, Vol. 18, No. 10, pp. 1117-1125.

Nonomura, T., Kubo, T., Oka, T., Shimoke, K., Yamada, M., Enokido, Y. & Hatanaka, H. (1996) Signaling pathways and survival effects of BDNF and NT-3 on cultured cerebellar granule cells. *Dev. Brain Res.*, Vol. 97, No. 1, 42-50.

Park, I.H., Arora, N., Huo, H., Maherali, N, Ahfeldt, T., Shimamura, A., Lensch, M.W., Cowan, C., Hochedlinger, K. & Daley, G.Q. (2008) Disease-Specific Induced Pluripotent Stem Cells. *Cell*, Vol. 134, No. 5, pp. 877-886.

Pelkmans, L., Fava, E., Grabner, H., Hannus, M., Habermann, B., Krausz, E. & Zerial M. (2005) Genome-wide analysis of human kinases in clathrin- and caveolae/raft-mediated endocytosis. *Nature*, Vol. 436, No. 7047, pp. 78-86.

Pepperkok, R., & Ellenberg, J. (2006) High-throughput fluorescence microscopy for systems biology. *Nature Rev Mol Cell Biol*, Vol. 7, No. 9, pp.690-696.

Pfeifer, M.J. & Scheel, G. (2009) Long-term storage of compound solutions for high-throughput screening by using a novel 1536-well microplate. *J. Biomol. Screen.*, Vol. 14, No. 5, pp. 492-498.

Rämö, P., Sacher, R., Snijder, B., Begemann, B., Pelkmans, L. (2009) CellClassifier: supervised learning of cellular phenotypes. Bioinformatics, Vol. 25, No. 22, pp. 3028–3030.

Rantamäki, T., Hendolin, P., Kankaanpää, A., Mijatovic, J., Piepponen, P., Domenici, E., Chao, M.V., Männistö, P.T. & Castrén, E. (2007) Pharmacologically diverse antidepressants rapidly activate brain-derived neurotrophic factor receptor TrkB and induce phospholipase-Cγ signalling pathways in mouse brain. *Neuropsychopharmacol.*, Vol. 32, No. 10, pp.2152-2162.

Schmitz, M.H., Held, M., Janssens, V., Hutchins, J.R., Hudecz, O., Ivanova, E., Goris, J., Trinkle-Mulcahy, L., Lamond, A.I., Poser, I., Hyman, A.A., Mechtler, K., Peters, J.M. & Gerlich, D.W. (2010) Live-cell imaging RNAi screen identifies PP2A-B55alpha and importin-beta1 as key mitotic exit regulators in human cells. *Nat. Cell Biol.*, Vol. 12, No. 9, pp. 886-893.

Segal, R.A., Pomeroy, S.L. & Stiles, C.D. (1995) Axonal growth and fasciculation linked to differential expression of BDNF and NT3 receptors in developing cerebellar granule cells. *J. Neurosci.*, Vol. 15, No. 7, pp. 4970-4981.

Simonen, M. & Gabriel, D. (2008) High-content screening as improved lead finding strategy. *Eur. Pharm. Rev.*, Vol. 13, No. 2, pp. 46-53.

Swedlow J.R., Goldberg, I., Brauer, E., & Sorger, P.K. (2003) Informatics and quantiative analysis in biological imaging. *Science*, Vol. 300, No. 5616, pp.100-102.

Unterreiner, V., Ibig-Rehm, Y., Simonen, M., Gubler, H. & Gabriel, D. (2009) Comparison of variability and sensitivity between nuclear translocation and luciferase reporter gene assays. *J. Biomol. Screen.*, Vol.14, No. 1, pp. 59-65.

Wang, D., Lagerstrom, R., Sun, C., Bishof, L., Vallotton, P. & Götte, M. (2010) HCA-Vision: Automated neurite outgrowth analysis. *J. Biomol. Screen.*, Vol.15, No. 9, pp. 1165-1170.

Yan, W.K., Goette, M. Hofmann, G., Zaror & I. Sim, J. (2009) High-level soluble expression, purification and characterization of active human midkine from Escherichia coli. *Protein Expr. Purif.*, Vol. 70, No. 2, pp. 270-276.

Young, D. W., Bender. A., Hoyt, J., McWhinnie, E., Chirn, G. W., Y; et al. (2008) Integrating high-content screening and ligand-target prediction identify mechanism of action. *Nat. Chem. Biol.*, Vol. 4, No. 1, pp. 59–68.

Drug Discovery and Development - Present and Future

Edited by Dr. Izet Kapetanović

Drug discovery and development process aims to make available medications that are safe and effective in improving the length and quality of life and relieving pain and suffering. However, the process is very complex, time consuming, resource intensive, requiring multi-disciplinary expertise and innovative approaches. There is a growing urgency to identify and develop more effective, efficient, and expedient ways to bring safe and effective products to the market. The drug discovery and development process relies on the utilization of relevant and robust tools, methods, models, and validated biomarkers that are predictive of clinical effects in terms of diagnosis, prevention, therapy, and prognosis. There is a growing emphasis on translational research, a bidirectional bench to the bedside approach, in an effort to improve the process efficiency and the need for further innovations. The authors in the book discuss the current and evolving state of drug discovery and development.

How to reference

In order to correctly reference this scholarly work, feel free to copy and paste the following:

INTECH
open science | open minds